



CELSR3 mRNA expression is increased in hepatocellular carcinoma and indicates poor prognosis

Xuefeng Gu^{1,2,*}, Hongbo Li^{3,*}, Ling Sha⁴, Yuan Mao⁵, Chuanbing Shi⁶ and Wei Zhao^{1,2}

¹ Medical School, Southeast University, Nanjing, Jiangsu, China

² The Second Hospital of Nanjing, Medical School, Southeast University, Nanjing, Jiangsu, China

³ Department of Hepatology, Infectious diseases Hospital Affiliated to Soochow University, Suzhou, Jiangsu, China

⁴ Department of Neurology, Affiliated Drum Tower Hospital of Nanjing University Medical School, Nanjing, Jiangsu, China

⁵ Department of Hematology and Oncology, Geriatric Hospital of Nanjing Medical University, Jiangsu Province Geriatric Hospital, Nanjing, Jiangsu, China

⁶ Department of Pathology, Pukou District Central Hospital, Pukou Branch of Jiangsu Province Hospital, The First Affiliated Hospital of Nanjing Medical University, Nanjing, Jiangsu, China

* These authors contributed equally to this work.

ABSTRACT

Objective. Hepatocellular carcinoma (HCC) is a disease that is associated with high mortality; currently, there is no curative and reliable treatment. Cadherin EGF LAG seven-pass G-type receptor 3 (CELSR3) is the key signaling molecule in the wingless and INT-1/planar cell polarity (WNT/PCP) pathway. This study aimed to elucidate the prognostic significance of CELSR3 in HCC patients.

Methods. The Cancer Genome Atlas (TCGA) database, the Cancer Cell Line Encyclopedia (CCLE) database and the Gene Expression Omnibus (GEO) database were used to analyze the expression of CELSR3 mRNA in HCC samples and cells. The relationship between CELSR3 mRNA and clinical features was assessed by the chi-square test. The diagnostic and predictive value of CELSR3 mRNA expression were analyzed using the receiver operating characteristic (ROC) curve. Kaplan–Meier curve and Cox regression analyses were performed to assess the prognostic value of CELSR3 mRNA in HCC patients. Finally, all three cohorts database was used for gene set enrichment analysis (GSEA) and the identification of CELSR3-related signal transduction pathways.

Results. The expression of CELSR3 mRNA was upregulated in HCC, and its expression was correlated with age ($P = 0.025$), tumor status ($P = 0.022$), clinical stage ($P = 0.003$), T classification ($P = 0.010$), vital status ($P = 0.001$), and relapse ($P = 0.005$). The ROC curve assessment indicated that CELSR3 mRNA expression has high diagnostic value in HCC and in the subgroup analysis of stage. In addition, the Kaplan–Meier curve and Cox analyses suggested that patients with high CELSR3 mRNA expression have a poor prognosis, indicating that CELSR3 mRNA is an independent prognostic factor for the overall survival of HCC patients. GSEA showed that GO somatic diversification of immune receptors, GO endonuclease activity, GO DNA repair complex and GO somatic cell DNA recombination, were differentially enriched in the meta-GEO cohort, the HCC cell line cohort and the TCGA cohort of the high CELSR3 mRNA expression phenotype.

Submitted 3 June 2019
Accepted 2 September 2019
Published 7 October 2019

Corresponding author
Wei Zhao, weizhaoseu@163.com

Academic editor
Vladimir Uversky

Additional Information and
Declarations can be found on
page 17

DOI 10.7717/peerj.7816

© Copyright
2019 Gu et al.

Distributed under
Creative Commons CC-BY 4.0

OPEN ACCESS

Conclusion. Our results indicate that CELSR3 mRNA is involved in the progression of cancer and can be used as a biomarker for the prognosis of HCC patients.

Subjects Bioinformatics, Gastroenterology and Hepatology, Oncology

Keywords GEO, The Cancer Genome Atlas, GSEA, HCC, CELSR3, CCLE

INTRODUCTION

Hepatocellular carcinoma (HCC) is currently one of the most common malignant tumors worldwide. Globally, the incidence rate is ranked 6th, and the mortality rate is ranked 4th among malignant tumors. There were approximately 840,000 newly diagnosed patients worldwide in 2018, and approximately 780,000 people die annually (*Bray et al., 2018*). Although the current treatment methods for HCC have made great progress, strategies for HCC treatment are still limited. Available studies have indicated that some genes are closely related to the prognosis of HCC and thus might be used as valuable biomarkers for the treatment of this disease (*Petrizzo et al., 2018*). Therefore, it is of great importance to search for markers of progression and poor prognosis of HCC.

As a calcium-dependent transmembrane glycoprotein, cadherin is characterized by an extracellular calcium-binding domain (composed of a sequence of approximately 110 repeated amino acids), and it plays important roles in embryonic development and synaptogenesis (*Gumbiner, 1996; Takeichi, 1991; Halbleib & Nelson, 2006; Takeichi, 2007*). The cadherin EGF LAG seven-pass G-type receptor (Celsr) gene family is related to nonclustered protocadherin (*Wu & Maniatis, 2000*). In mammals, evolution of the cadherin gene family led to three genes, CELSR1, Celsr2, and CELSR3 (*Beall, Boekelheide & Johnson, 2005; Formstone & Little, 2001; Tissir et al., 2002; Formstone & Mason, 2005*). CELSR3 is the key signaling molecule in the wingless and INT-1/planar cell polarity (WNT/PCP) pathway, an important pathway that controls the polarity of tissues and cell migration (*Katoh, 2005*). Recent studies (*Katoh & Katoh, 2007*) have shown that CELSR3 expression in adult brain tumors reflects the role of CELSR3 in carcinogenic processes. CELSR3 is selectively upregulated in pancreatic stellate cells (PSCs) of pancreatic tumors (*Erkan et al., 2010*). *Asad et al. (2014)* found that CELSR3 is highly expressed in ovarian cancer. *Pan et al. (2019)* constructed a ceRNA network in head and neck squamous cell carcinoma (HNSCC), and CELSR3 (as a differential gene of the ceRNA network) indicated a worse prognosis in the overall survival of HNSCC. *Xu et al. (2019)* compared normal cervical tissues and human papillomavirus (HPV) positive cervical cancer tissues and identified CELSR3 as a novel candidate gene related to the progression and carcinogenicity of cervical lesions. To determine the molecular basis of colorectal cancer (CRC) metastasis, Goryca et al. performed a whole-exome and genome-scale transcriptome sequencing of seven liver metastases and their matched primary tumors and normal tissues. The authors found that CELSR3 had exclusive metastatic variants (EMV) in four patients (*Goryca et al., 2018*).

However, there is still a lack of research on the prognostic value of CELSR3 in HCC. whether CELSR3 might also be a specific marker in liver tumors remains to be elucidated.

In this study, we evaluated the expression of CELSR3 mRNA in HCC, analyzed the relationship between CELSR3 mRNA expression and clinical features, and investigated the prognostic significance of CELSR3 mRNA in HCC patients. Finally, gene set enrichment analysis (GSEA) was performed to further explore the biological pathways by which CELSR3 participates in HCC pathogenesis.

This study demonstrates, for the first time, that CELSR3 is a prognostic gene of HCC and may represent a new potential marker associated with HCC progression. Furthermore, it is correlated with G1 pathway, ATRBRCA pathway, E2F targets, G2 M checkpoint and spermatogenesis. GO somatic diversification of immune receptors, GO endonuclease activity, GO DNA repair complex and GO somatic cell DNA recombination may be important biological pathways through which CELSR3 mRNA participates in the pathogenesis of liver cancer, which deserve further study.

MATERIALS AND METHODS

Data mining and collection

HCC patients in the TCGA and GEO cohorts meeting the following criteria were included in the study: (1) primary HCC samples (including hepatocellular carcinoma, hepatocholangiocarcinoma (mixed) and fibrolamellar carcinoma); (2) complete RNA-seq data. The exclusion criteria was samples that did not contain enough data for analysis. The gene expression data (423 cases, Workflow Type: HTSeq-Counts) and corresponding clinical information were obtained from The Cancer Genome Atlas (TCGA) Liver Hepatocellular Carcinoma (TCGA-LIHC) study of the official TCGA website (<https://cancergenome.nih.gov/>). The complete clinical data of the corresponding patients were obtained from cBioPortal (<http://www.cbioportal.org/>). A total of 373 HCC tissue specimens and 50 adjacent nontumor tissue specimens of HCC were included in the study. The Homo_sapiens.GRCh38.84.chr.gtf.gz file was downloaded from the Ensembl website (<https://asia.ensembl.org/index.html>), and ID conversion was performed using Perl (version 5.26.1). TCGA original HTSeq-Count data were processed using the Trimmed Mean of M-values (TMM) method for homogenization with edgeR. When an RNA had duplicate data, the average RNA expression was used. Microarray data were downloaded from the Gene Expression Omnibus (GEO) database. The [GSE54236](#) original Series Matrix dataset with survival data was based on the [GPL6480](#) (Agilent-014850 Whole Human Genome Microarray 4x44K G4112F, Agilent Technologies, CA, Palo Alto) (submission date: Jan 21, 2014). The [GSE60502](#) (submission date: Aug 18, 2014) datasets were based on [GPL570](#) (Affymetrix Human Genome U133A Array Affymetrix, Inc, CA, Santa Clara). [GSE41804](#) (submission date: Oct 24, 2012), [GSE45436](#) (submission date: Mar 22, 2013), [GSE62232](#) (submission date: Oct 09, 2014), and [GSE6764](#) (submission date: Jan 17, 2007) datasets, which were based on [GPL570](#) data (Affymetrix Human Genome U133 Plus 2.0 Array, Affymetrix, Inc, CA, Santa Clara). For the CEL expression profiles, Robust Multiarray Average (RMA) normalization was performed using the affy package. The expression level of CELSR3 mRNA was converted using the log₂ value for further analysis. The raw data in the dataset were annotated to obtain the gene expression levels and

the average expression values of probes were considered as the expression values of the corresponding genes. We combined the HCC microarray [GSE60502](#) and [GSE62232](#) in the GEO database using Perl (version 5.26.1) and performed batch normalization using the `sva` package of R. After combination and normalization, 99 HCC patients were divided into high and low expression groups according to the median value of CELSR3 expression for GSEA detection and verification. RNA expression (RNA-Seq) data for CELSR3 in established HCC cell lines were accessed on 01/02/19 ($n = 25$) from the Cancer Cell Line Encyclopedia (CCLE) database (<https://portals.broadinstitute.org/ccle/about>); RNA expression values were reported in reads per kilobase of transcript per million mapped reads (RPKM). We divided the expression of CELSR3 in the HCC cell lines into high and low expression groups using the median value, and then performed GSEA verification to observe the enrichment of CELSR3 differential expression in the HCC cell lines. The GSEA results were presented in the form of multiple GSEA using the `Plyr`, `grid`, `gridExtra` and `ggplot2` packages of R.

Gene set enrichment analysis

GSEA is a computational method that determines whether an a priori defined set of genes shows statistically significant, concordant differences between two biological states ([Subramanian et al., 2005](#)). In this study, HCC samples from TCGA data were divided into the CELSR3 high mRNA expression group and the low CELSR3 mRNA expression group based on the median value of CELSR3 mRNA expression. GSEA3.0 was adopted for GSEA. The functional gene set files “c2.cp.biocarta.v6.2.symbols.gmt”, “h.all.v6.2.symbols.gmt” and “c5.all.v6.2.symbols.gmt” were used to summarize and elucidate specific and well-defined biological states or processes. The number of substitutions per analysis was set at 1,000, and gene sets with $P < 0.05$ and a false discovery rate (FDR) < 0.25 were recognized as a significantly enriched.

Statistical analysis

SPSS statistical software, version 19.0 (SPSS Inc., Chicago, IL, USA) and STATA 12.0 (Stata Corporation, College Station, TX, USA) were used for statistical analysis. The `ggplot2` and `pROC` packages in the statistical software R ([R Core Team, 2018](#)) were used for graph generation. Discrete variables are expressed using a box plot to measure expression differences. The chi-square test was used to analyze the relationship between CELSR3 mRNA expression and clinical data. The Kaplan–Meier curve showed that clinicopathologic characteristics were associated with overall and relapse-free survival. Univariate Cox analysis was used to select relevant variables, and subsequently, multivariate Cox analysis was used for prognostic analysis of CELSR3 mRNA expression with regard to the overall and relapse-free survival (RFS) rate of HCC patients. The cutoff value was determined by the median value of CELSR3 mRNA expression. $P < 0.05$ was considered statistically significant.

Table 1 Clinical characteristics of the included patients.

| Characteristics | Number of sample size (%) |
|-------------------|---------------------------|
| Age (years) | |
| ≥60 | 203 (54.42) |
| <60 | 169 (45.31) |
| NA | 1 (0.27) |
| Gender | |
| Female | 121 (32.44) |
| Male | 252 (67.56) |
| Family history | |
| Yes | 112 (30.03) |
| No | 209 (56.03) |
| NA | 52 (13.94) |
| Tumor status | |
| With tumor | 112 (30.03) |
| Tumor free | 234 (62.73) |
| NA | 27 (7.24) |
| Radiation therapy | |
| No | 341 (91.42) |
| Yes | 9 (2.41) |
| NA | 23 (6.17) |
| Histologic grade | |
| Grade 1 | 55 (14.75) |
| Grade 2 | 178 (47.72) |
| Grade 3 | 123 (32.98) |
| Grade 4 | 12 (3.22) |
| NA | 5 (1.34) |
| Vascular invasion | |
| Macro | 16 (4.29) |
| Micro | 94 (25.20) |
| None | 207 (55.50) |
| NA | 56 (15.01) |
| TNM Stage | |
| Stage I | 172 (46.11) |
| Stage II | 87 (23.32) |
| Stage III | 85 (22.79) |
| Stage IV | 5 (1.34) |
| NA | 24 (6.43) |
| T classification | |
| T1 | 182 (48.79) |
| T2 | 95 (25.47) |
| T3 | 80 (21.45) |
| T4 | 13 (3.49) |

(continued on next page)

Table 1 (continued)

| Characteristics | Number of sample size (%) |
|------------------|---------------------------|
| TX | 1 (0.27) |
| NA | 2 (0.54) |
| N classification | |
| N0 | 253 (67.83) |
| N1 | 4 (1.07) |
| NX | 115 (30.83) |
| NA | 1 (0.27) |
| M classification | |
| M0 | 267 (71.58) |
| M1 | 4 (1.07) |
| MX | 102 (27.35) |
| Residual tumor | |
| R0 | 326 (87.40) |
| R1 | 17 (4.56) |
| R2 | 1 (0.27) |
| RX | 22 (5.90) |
| NA | 7 (1.88) |
| Vital status | |
| Living | 243 (65.15) |
| Deceased | 130 (34.85) |
| Relapse | |
| Yes | 176 (47.18) |
| No | 146 (39.14) |
| NA | 51 (13.67) |

Notes.

NA, not available; T, tumor stage; N, node; M, metastasis.

RESULTS

Patient characteristics

The clinical and gene expression data for the 373 cases of primary HCC were downloaded from TCGA. As shown in [Table 1](#), the median age at diagnosis was 61 years. In our study cohort, after excluding data that is not available, 14.9% of the tumors were well differentiated, 48.4% were moderately differentiated, and 36.7% were poorly or not differentiated. The tumor status included 234 cases without tumors (67.6%) and 112 cases with tumors (32.4%). There were 172 cases (49.3%) of stage I primary HCC, 87 cases (24.9%) of stage II HCC, 85 cases (24.4%) of stage III HCC, and 5 cases (1.4%) of stage IV HCC. There were 326 cases without and 18 with residual tumors. Of the subjects who were alive at the last follow-up, the median survival time was 19.42 months (range: 0-120.73 months).

High CELSR3 mRNA expression in HCC

HCC tissues and normal control tissues in TCGA data were compared using a box plot. As shown in [Fig. 1A](#), the expression of CELSR3 mRNA was higher in HCC tissues ($P = 0.000$). Moreover, there were also different CELSR3 expression levels in the groups classified

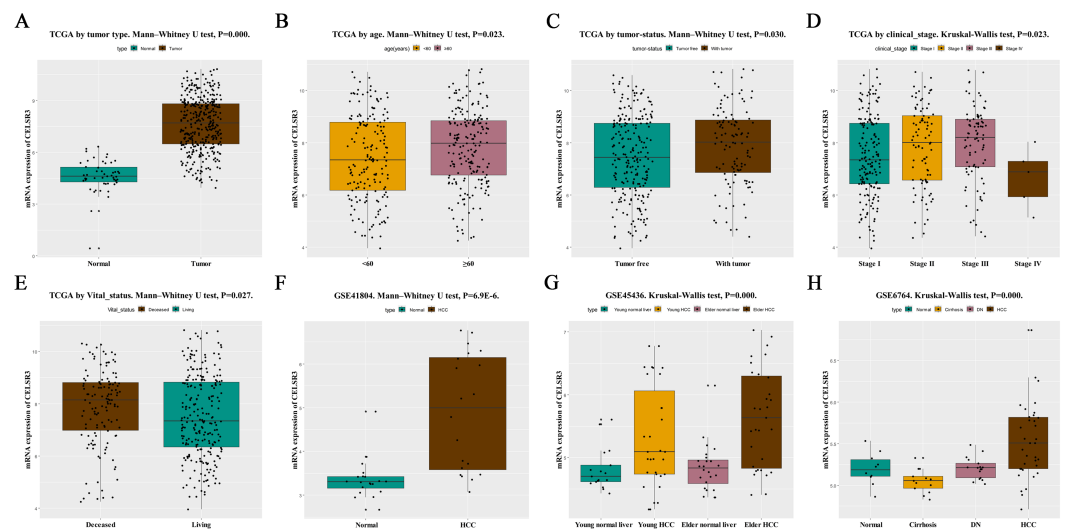


Figure 1 The relationship between CELSR3 mRNA expression and clinical features. Including (A) type, (B) age, (C) tumor status, (D) clinical stage, (E) vital status. The CELSR3 expression of HCC is compared with that in normal, elder/young, and cirrhosis/dysplastic nodule changes based on microarray [GSE41804](#) (F), [GSE45436](#) (G), and [GSE6764](#) (H). CELSR3, Cadherin EGF LAG seven-pass G-type receptor 3; TCGA, The Cancer Genome Atlas; HCC, hepatocellular carcinoma; DN, dysplastic nodule.

Full-size [DOI: 10.7717/peerj.7816/fig-1](https://doi.org/10.7717/peerj.7816/fig-1)

according to age (Fig. 1B, $P = 0.023$), tumor status (Fig. 1C, $P = 0.030$), stage (Fig. 1D, $P = 0.023$), and vital status (Fig. 1E, $P = 0.027$). The results indicated that CELSR3 is highly expressed in HCC tissues, and the expression of CELSR3 was high in older patients, in those with advanced tumor status or TNM stage III, and in those who had died. It is interesting to note that the expression of CELSR3 decreases in stage IV. When the GEO data were validated, CELSR3 mRNA expression differed for different types of liver tissues in the [GSE41804](#) (Fig. 1F, $P = 0.000$), [GSE45436](#) (Fig. 1G, $P = 0.000$), and [GSE6764](#) (Fig. 1H, $P = 0.000$) datasets. It is worth noting that the expression of CELSR3 mRNA in liver cirrhosis tissues was lower than in normal and HCC tissues.

Diagnostic function of CELSR3 mRNA

To verify the diagnostic value of CELSR3 in HCC, the ROC curve was used to analyze the AUC of CELSR3 expression associated with clinical pathological parameters of different HCC patients. As shown in Fig. 2A, CELSR3 could effectively distinguish normal liver tissue from HCC tissue. In the receiver operating characteristic (ROC) curve analysis of CELSR3, the area under the curve (AUC) was 0.954, indicating high diagnostic and predictive values of CELSR3. Furthermore, we performed ROC curve analysis of CELSR3 expression in different TNM stage subgroups of HCC patients; our results indicate that high expression of CELSR3 may be a promising diagnostic marker. In the subgroup analysis of stage, the diagnostic values at different stages were also high (AUC: stage I = 0.946; stage II = 0.964; stage III = 0.967; stage IV = 0.936; Figs. 2B–2E).

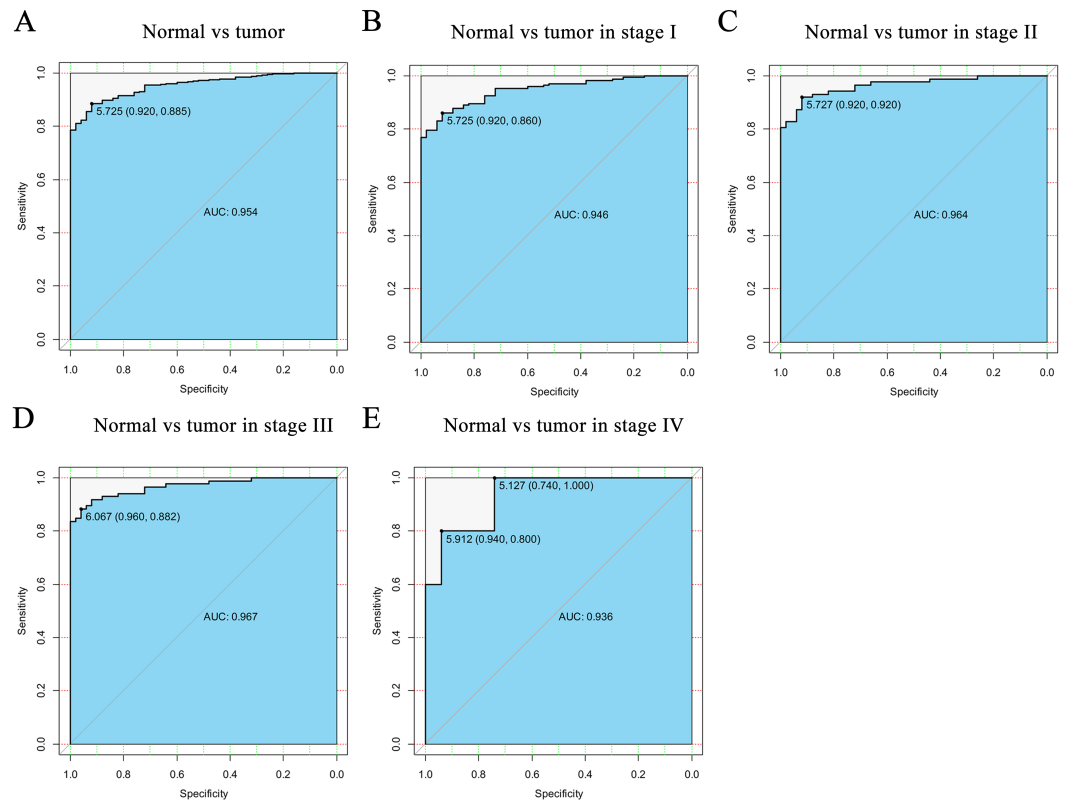


Figure 2 The ROC curve of CELSR3 in LIHC cohort. (A) Nontumor sample and tumor sample. (B) Nontumor sample and tumor sample of stage I. (C) Nontumor sample and tumor sample of stage II. (D) Nontumor sample and tumor sample of stage III. (E) Nontumor sample and tumor sample of stage IV. AUC, area under the curve; ROC, receiver-operating characteristic curve; LIHC, liver hepatocellular carcinoma.

Full-size DOI: 10.7717/peerj.7816/fig-2

Relationship between CELSR3 mRNA expression and clinical features of HCC

To validate the relationship between CELSR3 expression and clinical pathological features in HCC patients, we further analyzed the expression level of CELSR3 in HCC patients at different clinical stages. As shown in Table 2, the relationship between CELSR3 mRNA expression and clinical features indicated that CELSR3 mRNA expression was significantly correlated with age ($P = 0.025$), tumor status ($P = 0.022$), clinical stage ($P = 0.003$), T classification ($P = 0.010$), vital status ($P = 0.001$), and relapse ($P = 0.005$). Collectively, these data indicate that the expression of CELSR3 is associated with various important clinical pathological features of HCC.

Survival results and multivariate analysis

The Kaplan–Meier survival curve and log-rank test were used to evaluate the relationship between CELSR3 mRNA expression and overall (Fig. 3) and relapse-free survival (Fig. 4). All HCC patients were divided into either the CELSR3 high expression group or CELSR3 low expression group based on the median value of CELSR3 mRNA. We analyzed the OS

Table 2 Correlation between the clinicopathologic variables and CELSR3 mRNA expression in liver cancer.

| Parameters | Groups | N | CELSR3 expression | | | | χ^2 | P value |
|-------------------|------------|-----|-------------------|-------|-----|-------|----------|---------|
| | | | High | % | Low | % | | |
| Age (years) | ≥ 60 | 203 | 110 | 49.77 | 93 | 61.59 | 5.052 | 0.025* |
| | <60 | 169 | 111 | 50.23 | 58 | 38.41 | | |
| Gender | Female | 121 | 57 | 30.48 | 64 | 34.41 | 0.656 | 0.418 |
| | Male | 252 | 130 | 69.52 | 122 | 65.59 | | |
| Family history | Yes | 112 | 54 | 33.96 | 58 | 35.80 | 0.120 | 0.729 |
| | No | 209 | 105 | 66.04 | 104 | 64.20 | | |
| Tumor status | With tumor | 112 | 65 | 38.24 | 47 | 26.70 | 5.252 | 0.022* |
| | Tumor free | 234 | 105 | 61.76 | 129 | 73.30 | | |
| Radiation therapy | No | 341 | 173 | 97.74 | 168 | 97.11 | 0.139 | 0.71 |
| | Yes | 9 | 4 | 2.26 | 5 | 2.89 | | |
| Histologic grade | Grade 1 | 55 | 24 | 12.90 | 31 | 17.03 | 2.187 | 0.534 |
| | Grade 2 | 178 | 90 | 48.39 | 88 | 48.35 | | |
| | Grade 3 | 123 | 67 | 36.02 | 56 | 30.77 | | |
| | Grade 4 | 12 | 5 | 2.69 | 7 | 3.85 | | |
| Vascular invasion | Macro | 16 | 8 | 5.19 | 8 | 4.91 | 0.136 | 0.934 |
| | Micro | 94 | 47 | 30.52 | 47 | 28.83 | | |
| | None | 207 | 99 | 64.29 | 108 | 66.26 | | |
| TNM Stage | Stage I | 172 | 73 | 40.78 | 99 | 58.24 | 14.317 | 0.003* |
| | Stage II | 87 | 51 | 28.49 | 36 | 21.18 | | |
| | Stage III | 85 | 54 | 30.17 | 31 | 18.24 | | |
| | Stage IV | 5 | 1 | 0.56 | 4 | 2.35 | | |
| T classification | T1 | 182 | 76 | 40.64 | 106 | 57.61 | 13.367 | 0.010* |
| | T2 | 95 | 55 | 29.41 | 40 | 21.74 | | |
| | T3 | 80 | 50 | 26.74 | 30 | 16.3 | | |
| | T4 | 13 | 6 | 3.21 | 7 | 3.80 | | |
| | TX | 1 | 0 | 0.00 | 1 | 0.54 | | |
| N classification | N0 | 253 | 131 | 70.43 | 122 | 65.59 | 1.025 | 0.599 |
| | N1 | 4 | 2 | 1.08 | 2 | 1.08 | | |
| | NX | 115 | 53 | 28.49 | 62 | 33.33 | | |
| M classification | M0 | 267 | 134 | 71.66 | 133 | 71.51 | 1.040 | 0.594 |
| | M1 | 4 | 1 | 0.53 | 3 | 1.61 | | |
| | MX | 102 | 52 | 27.81 | 50 | 26.88 | | |
| Residual tumor | R0 | 326 | 165 | 89.67 | 161 | 88.46 | 1.097 | 0.778 |
| | R1 | 17 | 8 | 4.35 | 9 | 4.95 | | |
| | R2 | 1 | 0 | 0.00 | 1 | 0.55 | | |
| | RX | 22 | 11 | 5.98 | 11 | 6.04 | | |
| Vital status | Living | 243 | 107 | 57.22 | 136 | 73.12 | 10.381 | 0.001* |
| | Deceased | 130 | 80 | 42.78 | 50 | 26.88 | | |
| Relapse | Yes | 176 | 101 | 62.35 | 75 | 46.88 | 7.774 | 0.005* |
| | No | 146 | 61 | 37.65 | 85 | 53.12 | | |

Notes.* $P < 0.05$.

CELSR3, Cadherin EGF LAG seven-pass G-type receptor 3.

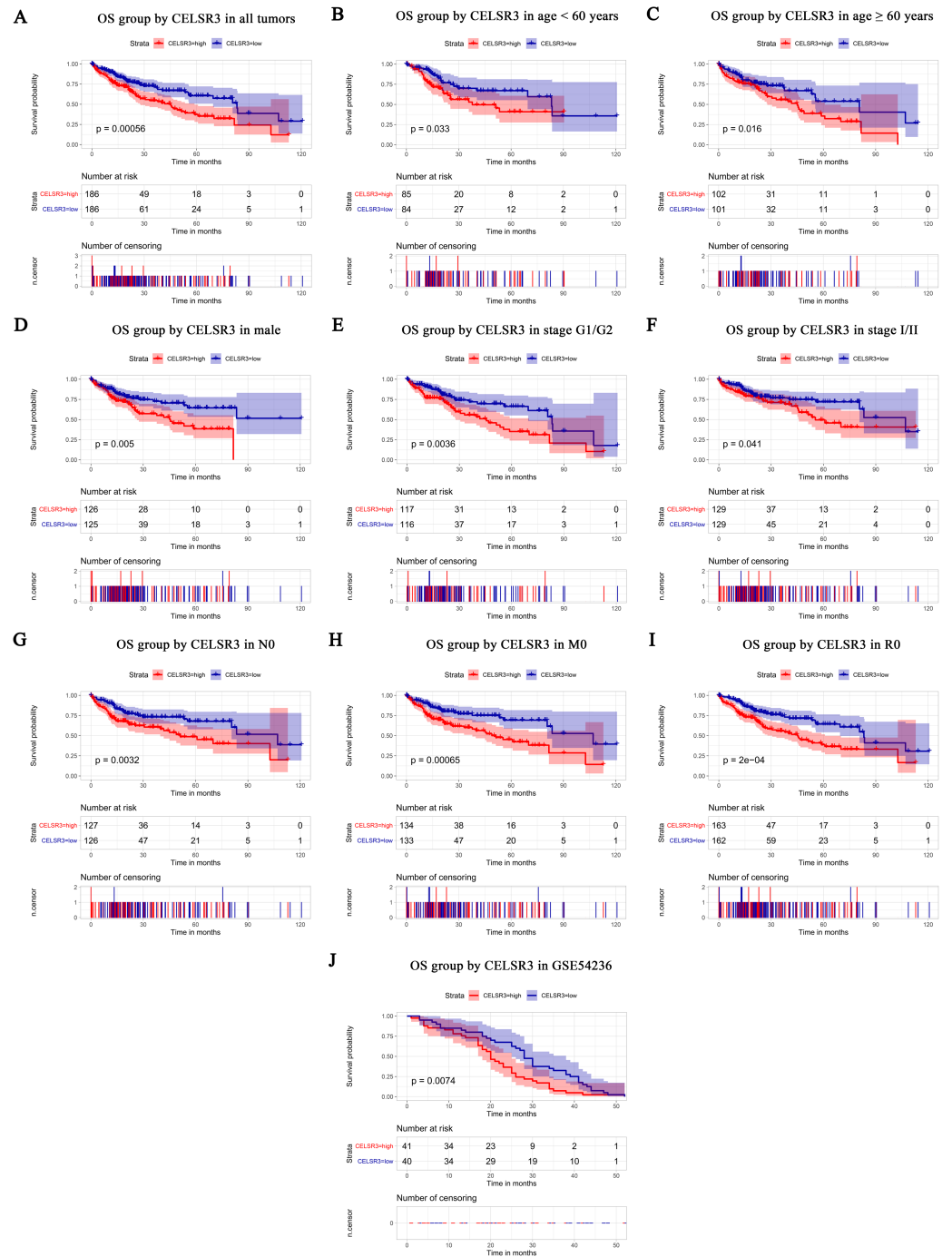


Figure 3 Survival analysis of CELSR3 expression level in terms of overall survival (OS). The OS values were analyzed in regards to the mRNA expression level of CELSR3 in all tumors and subgroups of HCC patients. OS analysis of (A) all tumors, (B) age < 60 years, (C) age ≥ 60 years, (D) male, (E) G1 + G2 stage, (F) stage I/II, (G) N0 stage, (H) M0 stage, and (I) R0 stage. Validation group of survival analysis in GSE54236 (J). OS: overall survival; T, tumor stage; N, node; M, metastasis; R, Residual tumor; HCC, hepatocellular carcinoma.

Full-size DOI: 10.7717/peerj.7816/fig-3

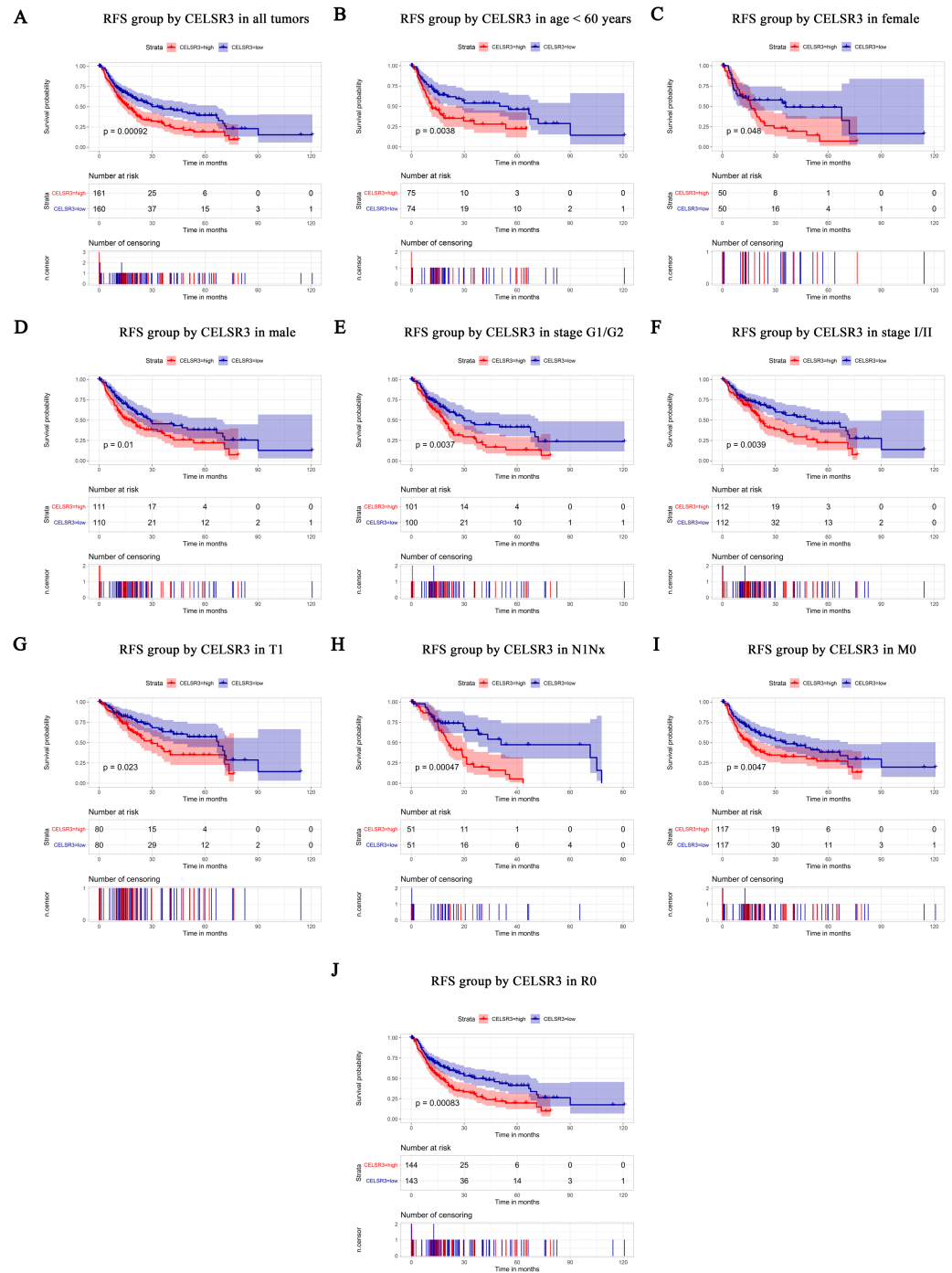


Figure 4 Survival analysis of CELSR3 expression in terms of relapse-free survival (RFS). The RFS values were analyzed in regards to the mRNA expression level of CELSR3 in all tumors and subgroups of HCC patients. RFS analysis of (A) all tumors, (B) age < 60 years, (C) age \geq 60 years, (D) male, (E) G1 + G2 stage, (F) stage I/II, (G) T1 stage, (H) N1Nx stage, (I) M0 stage, and (J) R0 stage. RFS, relapse-free survival.

Full-size DOI: 10.7717/peerj.7816/fig-4

time of 372 patients. The result showed that the overall survival was poor in patients with high CELSR3 mRNA expression (Fig. 3A; $P = 0.000$). Unexpectedly, RFS analysis produced similar results (Fig. 4A; $P = 0.000$). These results indicated that high CELSR3 expression in patients with HCC can predict a poor prognosis. To further confirm the prognostic value of CELSR3 in patients with HCC, we performed OS and RFS analysis in subgroups of HCC patients. The subgroup analysis indicated that the overall survival was poor in patients with high CELSR3 mRNA expression and an age <60 years or ≥ 60 years, male sex, histological grade G1/G2, stage I/II, N0 stage, M0 stage, and R0 stage (Figs. 3B–3I), and relapse-free survival was poor in the group with high CELSR3 mRNA expression and an age <60 years, female sex or male sex, histological grades G1/G2, stage I/II, T1 stage, N1Nx stage, M0 stage, and R0 stage (Figs. 4B–4J). The survival analysis validated by the GSE54236 data is shown in Fig. 3J ($P = 0.007$). These results demonstrated that high expression of CELSR3 can function as a prognostic biomarker of OS and RFS in subgroups of HCC patients. In different clinical subgroups of HCC patients, the prognostic value of CELSR3 varies, which can guide our clinical practice and deserves further study.

Univariate analysis showed that high expression of CELSR3 mRNA was significantly correlated with poor overall survival and other variables associated with a reduced overall survival rate, including tumor status, stage, T stage, N stage, M stage, and residual tumor. Multivariate analysis using the Cox proportional hazards model indicated that high expression of CELSR3 mRNA (HR = 1.88, $P = 0.004$) and residual tumor (HR = 1.36, $P = 0.033$) were independent prognostic factors for the overall survival of HCC patients (Table 3).

Identification of CELSR3-related signal transduction pathways by GSEA using TCGA cohort

To identify the differentially activated signaling pathways in HCC, gene expression enrichment analysis was performed between datasets with low or high CELSR3 mRNA expression. GSEA revealed significant differences (FDR < 0.25 , NOM P -value < 0.05) in the enrichment of the MSigDB Collection (c2.cp.biocarta.v6.2.symbols.gmt, h.all.v6.2.symbols.gmt, and c5.all.v6.2.symbols.gmt). Based on the normalized enrichment scores (NESs), the most significantly enriched signal transduction pathways were selected (Figs. 5A–5C; Tables 4 and 5). Figures 5A–5C shows that the cell cycle pathway, MCM pathway, ATR and BRCA pathway, ATM pathway, biocarta G1 pathway, E2F targets, hallmark G2/M checkpoint, and spermatogenesis, etc., were differentially enriched in phenotypes with high CELSR3 expression.

Validation using meta-GEO HCC cohort from GEO database and cell line data from CCLE

A total of 99 HCC specimens were obtained after combining the GSE60502 and GSE62232 microarray and batch normalization treatment. We performed enrichment analysis of meta-GEO HCC cohort data and cell line data. The results showed that after choosing the c2.cp.biocarta.v6.2.symbols.gmt gene set, two common enriched pathways,

biocarta G1 pathway, ATR and BRCA pathway, were present in both the meta-GEO cohort and the TCGA cohort of the high CELSR3 mRNA expression phenotype (Fig. 5D;

Table 3 Univariate and multivariate analyses of overall survival in patients with liver cancer.

| Variable | Univariate analysis | | | Multivariate analysis | | |
|--|---------------------|---------|-------------|-----------------------|---------|-------------|
| | HR | p value | 95% CI | HR | p value | 95% CI |
| CELSR3 expression (high/low) | 1.85 | 0.001* | 1.296–2.629 | 1.88 | 0.004* | 1.227–2.883 |
| Age, years (≥ 60 / <60) | 1.19 | 0.339 | 0.836–1.683 | | | |
| Gender (male/female) | 0.80 | 0.218 | 0.562–1.141 | | | |
| Family history of cancer (yes/no) | 1.19 | 0.349 | 0.826–1.721 | | | |
| Tumor status (with tumor/tumor free) | 1.53 | 0.021* | 1.068–2.200 | 1.14 | 0.544 | 0.750–1.724 |
| Radiation therapy (no/yes) | 0.91 | 0.869 | 0.288–2.861 | | | |
| Histological type (hepatocholangio carcinoma/hepatocellular/fibrolamellar) | 0.45 | 0.37 | 0.077–2.605 | | | |
| Histologic grade ((G4/G3/G2/G1)) | 1.11 | 0.368 | 0.881–1.408 | | | |
| Vascular invasion (Macro/Micro/None) | 1.36 | 0.063 | 0.984–1.888 | | | |
| Stage ((IV/III/II/I)) | 1.67 | 0.000* | 1.361–2.048 | 1.06 | 0.919 | 0.373–2.986 |
| T classification (TX/T4/T3/T2/T1) | 1.64 | 0.000* | 1.380–1.939 | 1.43 | 0.481 | 0.525–3.918 |
| N classification (NX/N1/N0) | 1.21 | 0.040* | 1.009–1.459 | 1.01 | 0.933 | 0.763–1.342 |
| M classification (MX0/M1/M0) | 1.26 | 0.013* | 1.050–1.518 | 1.17 | 0.297 | 0.869–1.585 |
| Residual tumor (RX/R2/R1/R0) | 1.48 | 0.001* | 1.1791.866 | 1.36 | 0.033* | 1.026–1.799 |

Notes.* $P < 0.05$.

HR, hazard ratio; CI, Confidence interval.

Table 4). After choosing the h.all.v6.2.symbols.gmt gene set, there were two common enriched pathways, hallmark G2/M checkpoint and hallmark spermatogenesis, in the meta-GEO cohort and the TCGA cohort of the high CELSR3 mRNA expression phenotype (**Fig. 5E**; **Table 4**), and one common enriched pathway, hallmark DNA repair, in the meta-GEO cohort and the HCC cell line cohort of the high CELSR3 mRNA expression phenotype (**Fig. 5G**; **Table 4**). After choosing the c5.all.v6.2.symbols.gmt gene set, four pathways, GO somatic diversification of immune receptors, GO endonuclease activity, GO DNA repair complex and GO somatic cell DNA recombination, were differentially enriched in the meta-GEO cohort, the HCC cell line cohort and the TCGA cohort of the high CELSR3 mRNA expression phenotype (**Figs. 5C, 5F, 5H**; **Table 5**).

DISCUSSION

This study confirmed the importance of CELSR3 in HCC and indicated that CELSR3 might serve as a biomarker of the prognosis of HCC. It also showed that high expression of CELSR3 in HCC was correlated with the age, tumor status, TNM staging, T staging, vital status, and relapse of HCC patients.

In recent years, studies examining CELSR3 have mainly focused on the effects of CELSR3 on the function of the nervous system (*Zhou et al., 2009*; *Zhou et al., 2008*; *Zhou, Goffinet & Tissir, 2008*) because proteins play an important role in the migration of neurons in the cortex and in the development of neuronal axons and dendrites. Recently, a relationship between CELSR3 expression and tumors, such as adult brain tumor (*Katoh & Katoh, 2007*) and ovarian cancer (*Asad et al., 2014*), has also been reported. Our study showed that

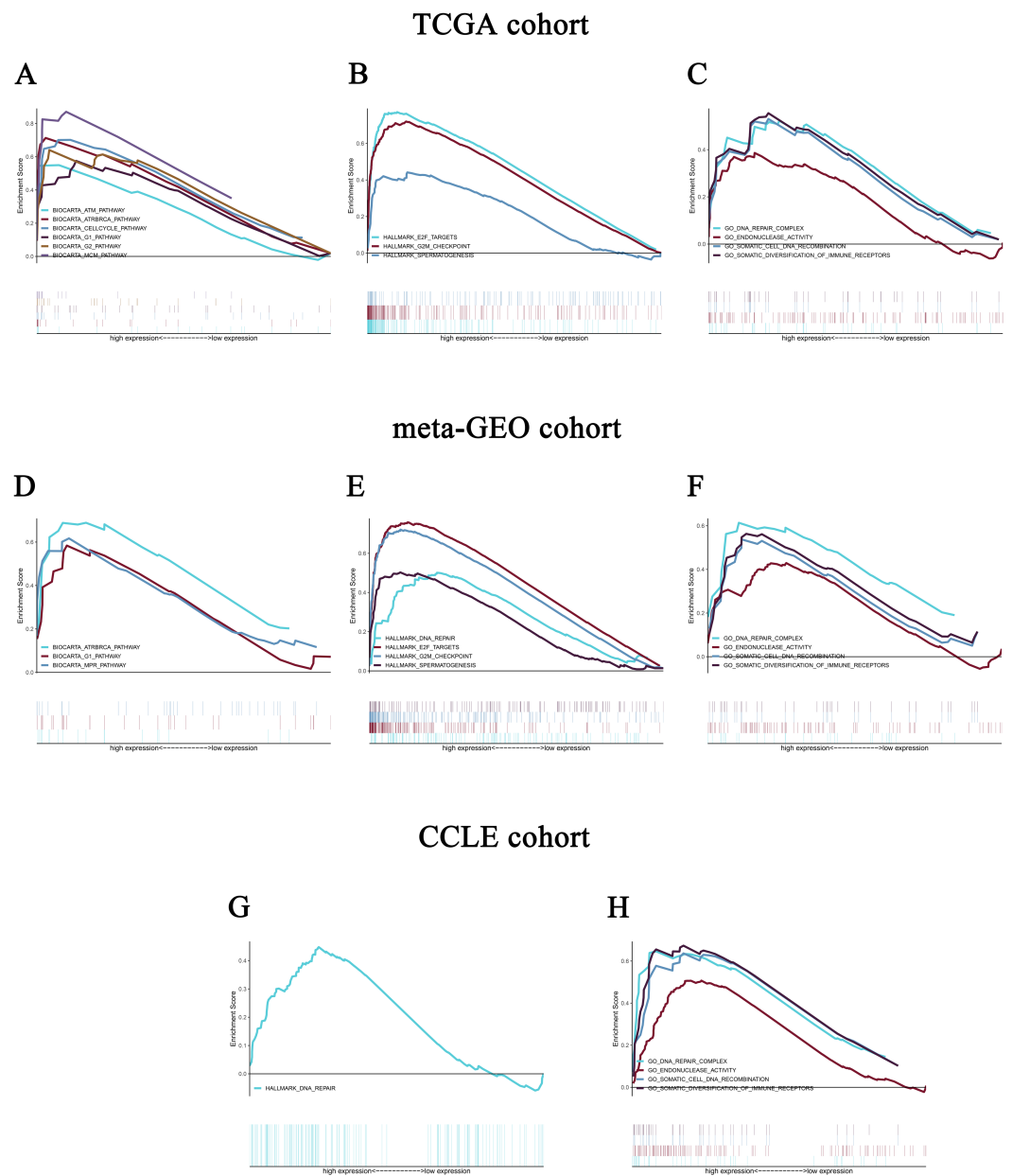


Figure 5 Enrichment plots from gene set enrichment analysis (GSEA). GSEA revealed significant differences in the enrichment of (A) c2.cp.biocarta.v6.2.symbols.gmt, (B) h.all.v6.2.symbols.gmt, and (C) c5.all.v6.2.symbols.gmt in the TCGA cohort. Validation using meta-GEO HCC cohort in the enrichment of (D) c2.cp.biocarta.v6.2.symbols.gmt, (E) h.all.v6.2.symbols.gmt, and (F) c5.all.v6.2.symbols.gmt. Validation using CCLC cohort in the enrichment of (G) h.all.v6.2.symbols.gmt, and (H) c5.all.v6.2.symbols.gmt. GSEA: gene set enrichment analysis; GEO: Gene Expression Omnibus; CCLC: Cancer Cell Line Encyclopedia.

Full-size DOI: 10.7717/peerj.7816/fig-5

Table 4 Gene sets enriched in phenotype high.

| MSigDB collection | Gene set name | NES | NOM <i>p</i> -value | FDR <i>q</i> -value |
|---------------------------------|----------------------------|-------|---------------------|---------------------|
| c2.cp.biocarta.v6.2.symbols.gmt | | | | |
| TCGA HCC cohort | BIOCARTA_CELLCYCLE_PATHWAY | 2.051 | 0.000 | 0.011 |
| | BIOCARTA_MCM_PATHWAY | 2.051 | 0.002 | 0.005 |
| | BIOCARTA_G2_PATHWAY | 1.887 | 0.008 | 0.033 |
| | BIOCARTA_ATRBRCA_PATHWAY | 1.879 | 0.008 | 0.026 |
| | BIOCARTA_G1_PATHWAY | 1.729 | 0.006 | 0.089 |
| | BIOCARTA_ATM_PATHWAY | 1.613 | 0.029 | 0.179 |
| meta-GEO HCC cohort | BIOCARTA_MPR_PATHWAY | 1.722 | 0.006 | 0.159 |
| | BIOCARTA_G1_PATHWAY | 1.520 | 0.021 | 0.211 |
| | BIOCARTA_ATRBRCA_PATHWAY | 1.547 | 0.023 | 0.213 |
| CCLC | no | | | |
| h.all.v6.2.symbols.gmt | | | | |
| TCGA HCC cohort | HALLMARK_E2F_TARGETS | 2.228 | 0.000 | 0.000 |
| | HALLMARK_G2M_CHECKPOINT | 2.202 | 0.000 | 0.000 |
| | HALLMARK_SPERMATOGENESIS | 1.742 | 0.002 | 0.071 |
| meta-GEO HCC cohort | HALLMARK_E2F_TARGETS | 1.549 | 0.008 | 0.066 |
| | HALLMARK_DNA_REPAIR | 1.735 | 0.008 | 0.039 |
| | HALLMARK_G2M_CHECKPOINT | 1.565 | 0.016 | 0.095 |
| | HALLMARK_SPERMATOGENESIS | 1.560 | 0.017 | 0.075 |
| CCLC | HALLMARK_DNA_REPAIR | 1.456 | 0.045 | 0.226 |

Notes.

NES, normalized enrichment score; NOM, nominal; FDR, false discovery rate; TCGA, The Cancer Genome Atlas; GEO, Gene Expression Omnibus; CCLC, Cancer Cell Line Encyclopedia.

Gene sets with NOM *p*-val <0.05 and FDR *q*-val <0.25 are considered as significant.

CELSR3 mRNA was highly expressed in HCC, which is consistent with studies of other tumors. Interestingly, our study showed that CELSR3 mRNA was upregulated in stage I/II/III and downregulated in stage IV tumors, suggesting that CELSR3 mRNA might be differentially expressed at different stages. Alternately, the results might be due to the small sample size of stage IV patients (five cases), and thus, expanding the sample size might provide a more valid result. Because the expression of CELSR3 mRNA was higher in deceased than in surviving patients, the relationship between CELSR3 mRNA and survival must be further explored.

The role of CELSR3 in tumorigenesis and progression has also been studied. [Erkan et al. \(2010\)](#) suggested that tissue fibrosis is a component of chronic inflammation (liver and pancreas) and pancreatic cancer. Activated PSCs and hepatic stellate cells (HSCs) play critical roles in fibrogenesis. These researchers found that CELSR3 was selectively upregulated in stellate cells in pancreatic tumors and might provide a favorable treatment strategy for selectively targeting the tumor stroma. [Scarlett et al. \(2011\)](#) also observed the colocalized expression of CELSR3 with green fluorescent protein (GFP) in tumor-associated PSCs, suggesting that CELSR3 is a specific marker of circulation of bone marrow-derived (BMD) tumor-associated PSCs. In our study, the role of CELSR3 in tumorigenesis and proliferation might explain the relationship

Table 5 Gene sets enriched in phenotype high.

| MSigDB collection | Gene set name | NES | NOM <i>p</i> -value | FDR <i>q</i> -value |
|--|--|-------|------------------------|------------------------|
| c5.all.v6.2.symbols.gmt TCGA HCC cohort | GO_SOMATIC_DIVERSIFICATION_OF_IMMUNE_RECEPTORS | 1.843 | 0.013 | 0.032 |
| | GO_ENDONUCLEASE_ACTIVITY | 1.646 | 0.012 | 0.091 |
| | GO_DNA_REPAIR_COMPLEX | 1.787 | 0.024 | 0.044 |
| | GO_SOMATIC_CELL_DNA_RECOMBINATION | 1.644 | 0.036 | 0.092 |
| meta-GEO HCC cohort | GO_SOMATIC_DIVERSIFICATION_OF_IMMUNE_RECEPTORS | 1.706 | 0.018 | 0.087 |
| | GO_ENDONUCLEASE_ACTIVITY | 1.576 | 0.006 | 0.123 |
| | GO_DNA_REPAIR_COMPLEX | 1.759 | 0.006 | 0.086 |
| | GO_SOMATIC_CELL_DNA_RECOMBINATION | 1.548 | 0.039 | 0.134 |
| CCLE | GO_SOMATIC_DIVERSIFICATION_OF_IMMUNE_RECEPTORS | 1.693 | 0.000 | 0.181 |
| | GO_ENDONUCLEASE_ACTIVITY | 1.616 | 0.002 | 0.209 |
| | GO_DNA_REPAIR_COMPLEX | 1.598 | 0.010 | 0.212 |
| | GO_SOMATIC_CELL_DNA_RECOMBINATION | 1.602 | 0.014 | 0.219 |

CELSR3 is closely related to the prognosis of cancer. CELSR3 is hypermethylated in oral squamous cell carcinoma (OSCC) and can be used as a potential biomarker for the diagnosis, prognosis, and treatment of OSCC (*Khor et al., 2014*). *Karpathakis et al. (2016)* conducted a complete molecular identification of small intestinal neuroendocrine tumors (SINETs) and found that CELSR3 has a significant epigenetic mutation that might be a potential drug target. In this study, we found that patients with high CELSR3 mRNA expression had poor overall survival, especially those with histological grade G1/G2 and stage I/II, which might contribute to the precise treatment and precision targeting of HCC. Importantly, we found that CELSR3 mRNA was an independent prognostic factor for the overall survival of HCC patients and demonstrated its potential to become a biomarker for HCC. In addition, CELSR3 mRNA showed no independent prognostic significance for recurrence-free survival. However, in the subgroup analysis of histological grade G1/G2, stage I/II, and N1Nx, and M0 stages, the R0 stage was associated with a poor recurrence-free survival rate.

We performed double validation in tissue samples and cell lines for the enriched pathways of the CELSR3 high expression phenotype. The results showed that the CELSR3 high expression group showed gene enrichment in multiple different gene sets of the MSigDB database that were similar to those in the TCGA, GEO and CCLE databases. In the TCGA and GEO tissue samples, biocarta G1 pathway, ATR and BRCA pathway, E2F targets, hallmark G2/M checkpoint and hallmark spermatogenesis were differentially enriched in the CELSR3 high expression phenotype, while they were not differentially enriched in the CELSR3 high expression phenotype of the HCC cell line cohort. Whether this is related to different tissue specimens and cell lines deserves further study. Interestingly, hallmark DNA repair was differentially enriched in the CELSR3 high expression phenotype of the

meta-GEO cohort and HCC cell line cohort. It is particularly noteworthy that GO somatic diversification of immune receptors, GO endonuclease activity, GO DNA repair complex and GO somatic cell DNA recombination were differentially enriched in all three cohorts. These four pathways may be important biological pathways for the involvement of CELSR3 mRNA in the pathogenesis of liver cancer and deserve further in-depth investigation.

To our knowledge, this is the first study to demonstrate the important role of CELSR3 mRNA in the prognosis of HCC. In future analyses, additional clinical trials will be required to validate the corresponding results to reveal the prognostic value of CELSR3 mRNA in HCC.

CONCLUSION

Our study showed that the expression of CELSR3 mRNA was significantly increased in HCC and was correlated with some clinical features and a poor prognosis in patients. In addition, G1 pathway, ATRBRCA pathway, E2F targets, G2 M checkpoint and spermatogenesis may be the key pathways through which CELSR3 regulates liver cancer. GO somatic diversification of immune receptors, GO endonuclease activity, GO DNA repair complex and GO somatic cell DNA recombination were differentially enriched in both tissue specimens and the cell line cohort; these may be the pathways in which CELSR3 participates in the regulatory mechanism of HCC. Therefore, CELSR3 might be a valuable biomarker for HCC patients.

ADDITIONAL INFORMATION AND DECLARATIONS

Funding

The authors received no funding for this work.

Competing Interests

The authors declare there are no competing interests.

Author Contributions

- Xuefeng Gu performed the experiments, analyzed the data, prepared figures and/or tables, authored or reviewed drafts of the paper, approved the final draft.
- Hongbo Li performed the experiments, prepared figures and/or tables.
- Ling Sha analyzed the data, contributed reagents/materials/analysis tools, prepared figures and/or tables.
- Yuan Mao and Chuanbing Shi contributed reagents/materials/analysis tools.
- Wei Zhao conceived and designed the experiments, approved the final draft.

Data Availability

The following information was supplied regarding data availability:

The raw measurements are available in the [Supplemental Files](#).

Supplemental Information

Supplemental information for this article can be found online at <http://dx.doi.org/10.7717/peerj.7816#supplemental-information>.

REFERENCES

- Asad M, Wong MK, Tan TZ, Choolani M, Low J, Mori S, Virshup D, Thiery JP, Huang RY. 2014. FZD7 drives in vitro aggressiveness in Stem-A subtype of ovarian cancer via regulation of non-canonical Wnt/PCP pathway. *Cell Death & Disease* 5:e1346 DOI 10.1038/cddis.2014.302.
- Beall SA, Boekelheide K, Johnson KJ. 2005. Hybrid GPCR/cadherin (Celsr) proteins in rat testis are expressed with cell type specificity and exhibit differential Sertoli cell-germ cell adhesion activity. *Journal of Andrology* 26:529–538 DOI 10.2164/jandrol.05003.
- Bray F, Ferlay J, Soerjomataram I, Siegel RL, Torre LA, Jemal A. 2018. Global cancer statistics 2018: GLOBOCAN estimates of incidence and mortality worldwide for 36 cancers in 185 countries. *CA: A Cancer Journal for Clinicians* 68:394–424 DOI 10.3322/caac.21492.
- Erkan M, Weis N, Pan Z, Schwager C, Samkharadze T, Jiang X, Wirkner U, Giese NA, Ansoerge W, Debus J, Huber PE, Friess H, Abdollahi A, Kleeff J. 2010. Organ-, inflammation- and cancer specific transcriptional fingerprints of pancreatic and hepatic stellate cells. *Molecular Cancer* 9:88 DOI 10.1186/1476-4598-9-88.
- Formstone CJ, Little PF. 2001. The flamingo-related mouse Celsr family (CELSR1-3) genes exhibit distinct patterns of expression during embryonic development. *Mechanisms of Development* 109:91–94 DOI 10.1016/S0925-4773(01)00515-9.
- Formstone CJ, Mason I. 2005. Expression of the Celsr/flamingo homologue, c-fmi1, in the early avian embryo indicates a conserved role in neural tube closure and additional roles in asymmetry and somitogenesis. *Developmental Dynamics* 232:408–413 DOI 10.1002/dvdy.20228.
- Goryca K, Kulecka M, Paziewska A, Dabrowska M, Grzelak M, Skrzypczak M, Ginalski K, Mroz A, Rutkowski A, Paczkowska K, Mikula M, Ostrowski J. 2018. Exome scale map of genetic alterations promoting metastasis in colorectal cancer. *BMC Genetics* 19:85 DOI 10.1186/s12863-018-0673-0.
- Gumbiner BM. 1996. Cell adhesion: the molecular basis of tissue architecture and morphogenesis. *Cell* 84:345–357 DOI 10.1016/s0092-8674(00)81279-9.
- Halbleib JM, Nelson WJ. 2006. Cadherins in development: cell adhesion, sorting, and tissue morphogenesis. *Genes and Development* 20:3199–3214 DOI 10.1101/gad.1486806.
- Karpathakis A, Dibra H, Pipinikas C, Feber A, Morris T, Francis J, Oukrif D, Mandair D, Pericleous M, Mohmaduvash M, Serra S, Ogunbiyi O, Novelli M, Luong T, Asa SL, Kulke M, Toumpanakis C, Meyer T, Caplin M, Meyerson M, Beck S, Thirlwell C. 2016. Prognostic impact of novel molecular subtypes of small intestinal neuroendocrine tumor. *Clinical Cancer Research* 22:250–258 DOI 10.1158/1078-0432.ccr-15-0373.
- Katoh M. 2005. WNT/PCP signaling pathway and human cancer (review). *Oncology Reports* 14:1583–1588 DOI 10.3892/or.14.6.1583.

- Katoh M, Katoh M. 2007.** Comparative integromics on non-canonical WNT or planar cell polarity signaling molecules: transcriptional mechanism of PTK7 in colorectal cancer and that of SEMA6A in undifferentiated ES cells. *International Journal of Molecular Medicine* **20**:405–409 DOI [10.3892/ijmm.20.3.405](https://doi.org/10.3892/ijmm.20.3.405).
- Khor GH, Froemming GR, Zain RB, Abraham MT, Thong KL. 2014.** Screening of differential promoter hypermethylated genes in primary oral squamous cell carcinoma. *Asian Pacific Journal of Cancer Prevention* **15**:8957–8961 DOI [10.7314/apjcp.2014.15.20.8957](https://doi.org/10.7314/apjcp.2014.15.20.8957).
- Pan Y, Liu G, Wang D, Li Y. 2019.** Analysis of lncRNA-mediated ceRNA crosstalk and identification of prognostic signature in head and neck squamous cell carcinoma. *Frontiers in Pharmacology* **10**:150 DOI [10.3389/fphar.2019.00150](https://doi.org/10.3389/fphar.2019.00150).
- Petrizzo A, Mauriello A, Tornesello ML, Buonaguro FM, Tagliamonte M, Buonaguro L. 2018.** Cellular prognostic markers in hepatitis-related hepatocellular carcinoma. *Infect Agent Cancer* **13**:10 DOI [10.1186/s13027-018-0183-8](https://doi.org/10.1186/s13027-018-0183-8).
- R Core Team. 2018.** R: a language and environment for statistical computing. Version 3.5.2. Vienna: R Foundation for Statistical Computing. Available at <https://www.R-project.org/>.
- Scarlett CJ, Colvin EK, Pinese M, Chang DK, Morey AL, Musgrove EA, Pajic M, Apte M, Henshall SM, Sutherland RL, Kench JG, Biankin AV. 2011.** Recruitment and activation of pancreatic stellate cells from the bone marrow in pancreatic cancer: a model of tumor-host interaction. *PLOS ONE* **6**:e26088 DOI [10.1371/journal.pone.0026088](https://doi.org/10.1371/journal.pone.0026088).
- Subramanian A, Tamayo P, Mootha VK, Mukherjee S, Ebert BL, Gillette MA, Paulovich A, Pomeroy SL, Golub TR, Lander ES, Mesirov JP. 2005.** Gene set enrichment analysis: a knowledge-based approach for interpreting genome-wide expression profiles. *Proceedings of the National Academy of Sciences of the United States of America* **102**:15545–15550 DOI [10.1073/pnas.0506580102](https://doi.org/10.1073/pnas.0506580102).
- Takeichi M. 1991.** Cadherin cell adhesion receptors as a morphogenetic regulator. *Science* **251**:1451–1455 DOI [10.1126/science.2006419](https://doi.org/10.1126/science.2006419).
- Takeichi M. 2007.** The cadherin superfamily in neuronal connections and interactions. *Nature Reviews Neuroscience* **8**:11–20 DOI [10.1038/nrn2043](https://doi.org/10.1038/nrn2043).
- Tissir F, De-Backer O, Goffinet AM, Lambert de Rouvroit C. 2002.** Developmental expression profiles of Celsr (Flamingo) genes in the mouse. *Mechanisms of Development* **112**:157–160 DOI [10.1016/S0925-4773\(01\)00623-2](https://doi.org/10.1016/S0925-4773(01)00623-2).
- Wu Q, Maniatis T. 2000.** Large exons encoding multiple ectodomains are a characteristic feature of protocadherin genes. *Proceedings of the National Academy of Sciences of the United States of America* **97**:3124–3129 DOI [10.1073/pnas.060027397](https://doi.org/10.1073/pnas.060027397).
- Xu J, Liu H, Yang Y, Wang X, Liu P, Li Y, Meyers C, Banerjee NS, Wang HK, Cam M, Lu W, Chow LT. 2019.** Genome-wide profiling of cervical RNA-binding proteins identifies human papillomavirus regulation of RNASEH2A expression by viral E7 and E2F1. *MBio* **10**(1):e02687-18 DOI [10.1128/mBio.02687-18](https://doi.org/10.1128/mBio.02687-18).
- Zhou L, Bar I, Achouri Y, Campbell K, De Backer O, Hebert JM, Jones K, Kessar N, De Rouvroit CL, O’Leary D, Richardson WD, Goffinet AM, Tissir F. 2008.** Early

forebrain wiring: genetic dissection using conditional CELSR3 mutant mice. *Science* **320**:946–949 DOI [10.1126/science.1155244](https://doi.org/10.1126/science.1155244).

Zhou L, Goffinet AM, Tissir F. 2008. Role of the cadherin CELSR3 in the connectivity of the cerebral cortex. *Medecine sciences* **24**:1025–1027 DOI [10.1051/medsci/200824121025](https://doi.org/10.1051/medsci/200824121025).

Zhou L, Qu Y, Tissir F, Goffinet AM. 2009. Role of the atypical cadherin CELSR3 during development of the internal capsule. *Cereb Cortex* **19(Suppl 1)**:i114–i119 DOI [10.1093/cercor/bhp032](https://doi.org/10.1093/cercor/bhp032).